Solubilities of Inert Gases in Styrene-Butadiene-Styrene Block Copolymers

Hisashi ODANI, Kazuo TAIRA, Tetsuo YAMAGUCHI,
Norio NEMOTO, and Michio KURATA*

The solubility coefficients of helium, argon, and xenon in two SBS block copolymer samples having different domain structures were determined between 25 and 120°C by the desorption and the time-lag methods. In the first method after the equilibrium had been established between polymer and gas phase, the dissolved gas was desorbed into a known large volume, and the solubility coefficient S was evaluated. In the second method the time-lag solubility coefficient S_θ was calculated from the values of permeability and (time-lag) diffusion coefficients, which were obtained from permeability experiments. In the desorption process of the first method, the pressure increase in the desorption system was measured as a function of time, and the diffusion coefficient was estimated therefrom. For all systems over the pressure and temperature range studied, Henry's law was always obeyed, and little differences between two copolymer samples were observed. At lower temperatures the values of S were greater than those of S_θ. It was concluded that the time-lag method counts only the mobile penetrant molecule in the rubbery polybutadiene matrix, while the desorption method counts less diffusive species in the glassy polystyrene domains as well. In the temperature region below about 85°C the temperature dependence of the solubility coefficient was expressed well by the Arrhenius-type equation with a constant apparent heat of solution. The diffusion coefficient estimated from the desorption method agreed practically with that evaluated from the time lag of permeability measurements. The relationship between the logarithm of S at 25°C and the Lennard-Jones force constant ε/k of the gases was well expressed by a straight line. Also, the apparent heat of solution was linearly correlated with ε/k. The slopes of the both plots were found to be well compared with those predicted by the thermodynamic treatment developed by Michaels and Bixler. The product of the tortuosity factor and the chain immobilization factor was estimated from the observed diffusion, permeation, and solubility coefficients. It was found that the products for the sample, in which polystyrene rods dispersed in polybutadiene matrix, were smaller than those for the other sample having domain structure of alternating lamellae of styrene and butadiene components. The products for the latter sample increased with increasing the molecular size of the gas.

INTRODUCTION

In a previous paper[1] (referred to henceforth as Part I) the permeation and diffusion behavior of inert gases through styrene-butadiene-styrene (SBS) block copolymer was described. The observed values of permeability coefficients were well explained in terms of a simple model consisted of parallel array of elements of the respective component homopolymers. From the results, together with those of an analysis of the temperature dependence of diffusion coefficient, it has been suggested that, as far as the kinetic nature is concerned, the permeation and diffusion processes

---

* 小谷　寿, 平　和雄, 山口哲男, 根本紀夫, 倉田道夫 : Laboratory of Polymer Solution, Institute for Chemical Research, Kyoto University, Uji, Kyoto.

are governed primarily by those in rubbery polybutadiene matrix.

Since the permeability coefficient is a composite quantity, knowledge concerning solubilities of the gases, especially those at the sorption equilibrium, is required in order to obtain better understanding of the permeation process of the inert gases through the block copolymer films. Also, the knowledge will help us in getting useful information about microstructure of the block copolymer solids. This paper presents solubility data of inert gases in the SBS block copolymer samples. The solubilities have been measured by time-lag and static sorption methods. This work is complementary to the previous study of the permeation and diffusion, which was concerned with the dynamic nature of the process, and serves to elucidate the role of less diffusive polystyrene phases in the solution and transport processes.

EXPERIMENTAL

Materials

The SBS block copolymer samples employed were identical with those used in Part I.[1] The copolymer films having two different types of domain structures were used; (a) polystyrene rods dispersed in polybutadiene matrix (designated as R–1) and (b) alternating lamellae of styrene and butadiene components (L–1). Helium, argon, and xenon were used as penetrant. These gases were obtained from Takachiho Kagakukogyo, Co. Ltd., and the purity of each gas exceeded 99.995% by volume.

Methods
Measurements of the Solubility Coefficient.

Solubility coefficients were measured by two methods.

Time-lag Method. Having determined the permeability and diffusion coefficients from permeation experiments (see Part I), the solubility coefficient S_θ may be estimated through the relation

$$P = D_\theta S_\theta \qquad (1).$$

The permeability coefficient P is here expressed in terms of the volume of gas, expressed in cm^3 at STP (standard temperature and pressure), which permeates per second through 1 cm^2 of polymer film 1 cm thick for a pressure difference of 1 cm Hg. The diffusion coefficient D_θ is expressed in cm^2/sec. Therefore, the solubility coefficient S_θ is expressed in units of cubic centimeters of gas measured at STP in 1 cm^3 polymer when the pressure of the gas is 1 cm Hg. The subscript θ means that the diffusion coefficient is determined from the time lag for permeation and that the solubility coefficient is calculated therefrom using the relation (1).

Static Sorption Method. Measurements of the solubility coefficient by the static sorption method were performed using an apparatus similar to that employed by Meares.[2] The apparatus is shown schematically in Fig. 1. We used carefully-hand-ground taps in place of mercury cut-offs. Errors arising from solution of inert gases in tap grease, Apiezon high vacuum grease was used in this work, were found to
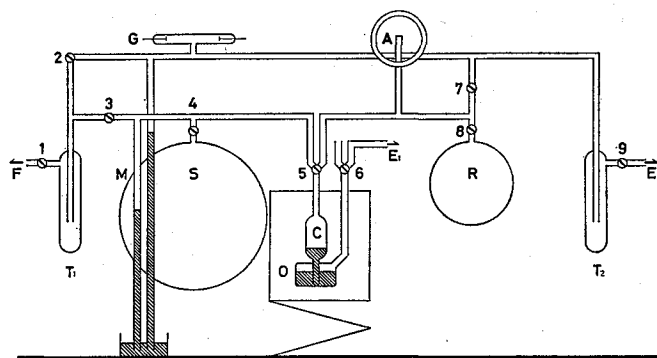
Fig. 1. The sorption apparatus. *S*, gas supply. *M*, gas-supply manometer. *C*, bulb (in which is placed the polymer sample). *O*, oil thermostat. *G*, Geisler tube. *A*, rotary McLeod gauge. *R*, Gas reservoir. T_1, gas-purification trap. *F*, to gas cylinder. E_1, to rotary mechanical pump. T_2, trap for oil diffusion pump. E_2, to oil diffusion pump and rotary mechanical forepump. 1–4 and 7–9, high vacuum taps. 5 and 6, two-way control taps.

be negligible compared with those originated from other sources such as the uncertainity involved in measurements of film thickness and the fluctuation in room temperature. The gas-supply system is enclosed by a tap 3 and a two-way control tap 5, and the desorption system is enclosed by the tap 5 and another tap 7. The former system is identical with the high pressure part of the permeability apparatus described in Part I. The main components in this system are the gas-supply monometer *M* and the gas-supply flask *S*. The polymer sample placed in a cage which is made from thin wire of platinum, is contained in the bulb *C*. In the bulb the cage, accordingly the polymer sample also, is tightly positioned by dimples pressed in the glass. The lower limb of the bulb is connected to the mercury reservior by means of a carefully-hand-ground joint. The desorption system is consisted of the rotary McLeod gauge *A* and the gas reservoir *R*.

The apparatus was operated as follows. The polymer sample, which had been annealed at a temperature 120°C for about three hours under high vacuum, was placed in the platinum cage, and the cage was installed in the bulb *C*. The mercury reservoir was then fixed to the bulb. The bulb and the mercury reservoir were immersed in the oil bath *O* by raising the bath with a laboratory jack. The temperature of the bath was regulated to ±0.2 and ±0.3°C in the temperature region 25 to 90°C and 95 to 120°C, respectively. After the whole apparatus had been thoroughly outgassed by prolonged pumping, the two-way control tap 5 was connected to the gas-supply system, and equilibrium established between the polymer and the gas phase. The equilibrium pressure was measured by observing the manometer *M* with a cathetometer.

After equilibrium, the dissolved gas was allowed to desorb from the polymer sample. By operating the two-way tap 6 mercury in the mercury reservoir was raised into the bore of the tap 5 through the bulb *C*. The tap was then turned to the closed position. The mercury was lowered through *C* to a mark etched at 5 mm below the dimples of *C*. To ensure that the gas surrounding the polymer sample had been

(411)

expelled as perfectly as possible before commencing the desorption procedure, Meares adopted the re-sweeping procedure.[2] In brief, after the tap 5 had been turned to the closed position the mercury was raised to the tap and the gas collected in the re-sweep was expelled to the gas-supply system. In our preliminary experiments, however, the procedure was found to be insufficient to remove a trace of gas trapped on glass wall and mercury. Accordingly we employed a procedure which was similar to that developed by Michaels and Parker in measuring solubility of gases in poly-ethylene.[3] After the tap 5 was opened to the desorption system, in which the taps 7 and 9 had been turned to the open position and the tap 8 to the closed position, the mercury lowered to the etched mark. Using an oil diffusion pump, which has a speed of exhaust of about 220 liters per second and an ultimate pressure of 10^{-7} mm Hg with a 400 r.p.m. rotary mechanical forepump, a pressure of less than 0.1 mm Hg was able to be attained within a one-minute pumping. The trapped gas was effectively removed by the pumping procedure, but the dissolved gas was also desorbed from the polymer film to a certain degree if the pumping interval was prolonged. Hence the pumping interval was empirically decided as follows. For example, in the system of xenon and L–1 a series of measurements was tested with the intervals ranged from 0.5 to 9 minutes, and a two-minute pumping was found to be suitable not only to ex-haust the trapped gas but also to keep in the ratio M_{ex}/M_{∞} as low as less than 0.3. Here, M_{ex} and M_{∞} are respectively amounts of the gas desorbed in the pumping inter-val and at infinite time.

After the exhaust procedure, the mercury was raised to cover enough the polymer sample by operating the tap 6. The pumping was continued until the desorption system had been out-gassed down to a pressure of about 10^{-6} mm Hg. The taps 7 and 8 in the desorption system were then turned respectively to the closed and the open positions. The mercury was again lowered to the etched mark, and the dissolved gas was allowed to desorb from the polymer sample. The final pressure in A was recorded with the room temperature. As described below, in the course of desorption the pressure increase of the desorption system was measured as a function of time and the diffusion coefficient was determined. In the measurement a stop-watch was started when the mercury was half-way down the bulb C.

The volume of the desorption system was determined by expansion experiment using helium. In the experiments a 500 ml flask was fixed to the apparatus in the place of the mercury reservoir by means of the glass joint, and the pressure in the gas-supply manometer was measured.

The solubility coefficient $S(p_0)$, expressed in units of cm³(STP) per cm³ polymer per cm Hg, is calculated by a material balance; that is,

$$76\,S(p_0)\,p_0 V_p = p_\infty (V + 76\,S(p_\infty) V_p) \qquad (2),$$

where p_0 is the equilibrium pressure, cm Hg, at the initial sorption equilibrium, p_∞ the final pressure at the desorption equilibrium, and V_p and V volumes of the polymer and the desorption system, respectively. In the present study, V was about 500 cm³ or 1000 cm³ and V_p's were from 0.05 to 1 cm³. Accordingly, the second term in the parentheses on the right hand side of the above equation can be neglected, and Eq. (2) reduces to

$$76 S(p_0) p_0 V_p = p_\infty V \qquad (3).$$

By taking into account of the amount of gas desorbed in the pumping interval, $S(p_0)$ can be expressed as

$$S(p_0) = \frac{p_\infty V}{76 p_0 V_p} \left(1 + \frac{M_{ex}}{M_\infty} \right) \qquad (4).$$

The correction term, M_{ex}/M_∞, was calculated by using the fundamental relations for diffusion described in the following section.

Estimation of the Diffusion Coefficient.

During the desorption procedure, by observing the pressure increase in the desorption system as a function of time, one may estimate the diffusion coefficient.

If the penetrant concentrations within the surfaces of an isopropic film of thickness, X, are maintained zero, the amount of penetrant, M_t, desorbed from the film in a time, t, may be written as follows: [4]

$$\frac{M_t}{M_\infty} = 1 - \frac{8}{\pi^2} \sum_{n=0}^{\infty} \frac{1}{(2n+1)^2} \exp\left\{ - \frac{D(2n+1)^2 \pi^2 t}{X^2} \right\} \qquad (5),$$

where M_∞ is the amount of penetrant desorbed at infinite time, and D is the diffusion coefficient. In this analysis, the desorption is considered to be a diffusion process controlled by a constant D. As described later this is the case for the system studied here. If I_d denotes the initial slope of the reduced desorption curve, $d(M_t/M_\infty)/d(t^{1/2}/X)$, then D is given by the expression [5]

$$D = \frac{\pi}{16} I_d^2 \qquad (6).$$

Two considerations arose in the estimation of D from the experimental results. The first concerned a positive intercept observed in the reduced desorption curve. An example is shown in Fig. 2. Though the plot at smaller values of $t^{1/2}/X$ is well represented by a straight line (a dotted line in Fig. 2), the line does not pass through the origin but exhibits the positive intercept at $t=0$. The trend was observed for all combinations of gas and block copolymer film studied. The real implication of the results is not known to us at present. As seen in Fig. 2, the magnitudes of the positive intercept were always very small fractions of the equilibrium value of the ordinate, unity. After having been subtracted the value of the intercept from the
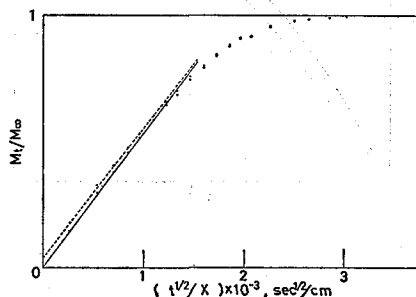

Fig. 2. Reduced desorption curves. ----●----, observed;
——●—— corrected for the positive intercept at $t=0$.

observed values of the amount of penetrant desorbed, the M_t/M_∞ versus $t^{1/2}/X$ plot was reconstructed. This plot for short times is represented also by a straight line (a solid line in Fig. 2), which is nearly parallel with the dotted line and passes the origin. The initial slope of the replotted curve was empirically adopted as I_d in Eq. (6), and D was calculated.

The second matter was a correction which should apply to results obtained with thicker films of the polymer. Equation (5), and Eq. (6) also, can apply in practice to diffusion into, or out of, a plane sheet so thin that effectively all the penetrant enters, or leaves, through the plane surfaces. Therefore, if a thicker film, in other words a sample better recognized as a block, is used in measurement, the amount of penetrant absorbed, or desorbed, through the edges of the polymer sample is no longer negligible and the process should be treated as the three-dimensional problem. If the diffusion process takes place in a rectangular parallelepiped whose edges are parallel to the axes of coordinates and are of lengths X, Y, and Z, the fundamental differential equation takes the form

$$\frac{\partial C}{\partial t} = D\left(\frac{\partial^2 C}{\partial x^2} + \frac{\partial^2 C}{\partial y^2} + \frac{\partial^2 C}{\partial z^2}\right) \tag{7}$$

provided that D is a constant. The solution of Eq. (7) is the product of the solutions of the three one-variable problems.[6] The expression for the amount of gas desorbed in a time t, which corresponds to Eq. (5) in the one-dimensional case, is then given[7]

$$\frac{M_t}{M_\infty} = 1 - \frac{512}{\pi^6} \sum_{l=0}^{\infty} \sum_{m=0}^{\infty} \sum_{n=0}^{\infty} \frac{1}{(2l+1)^2(2m+1)^2(2n+1)^2} \exp(-\alpha t) \tag{8}$$

with

$$\alpha = D\pi^2 \left\{ \frac{(2l+1)^2}{X^2} + \frac{(2m+1)^2}{Y^2} + \frac{(2n+1)^2}{Z^2} \right\} \tag{9}.$$

In Fig. 3, a comparison is made between the values of M_t/M_∞ calculated from Eqs. (8) and (5). In the example, D and X are identical for the two curves, but both Y and Z are different by a factor of 10^5. It is seen from the figure that the values of M_t/M_∞ for three-dimensional diffusion (a dotted line in Fig. 3) are always
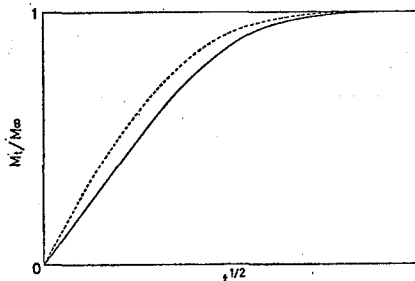

Fig. 3. Comparison between a calculated desorption curve for a semi-infinite film (——) and that for a rectangular parallelepiped (----). Dimensions of the semi-infinite film and those of the rectangular parallelepiped were $0.3 \times 10{,}000 \times 10{,}000$ cm³ and $0.3 \times 2 \times 1$ cm³, respectively. D was taken as 5×10^{-6} cm²/sec.

greater than those for one-dimensional diffusion. The initial linear region of the curve for the former diffusion is limited to less than a half of M_∞, while that for the latter is obtained over 60% or more of M_∞.

With the aid of the curves shown in Fig. 3, a correction factor, $F(XYZ)$, was determined by

$$F(XYZ) = \left(\frac{I_3}{I_1}\right)^2 \tag{10},$$

where I_1 and I_3 are the initial slopes of the curves calculated from Eqs. (5) and (8), respectively. The diffusion coefficient was then estimated through the relation

$$D = \frac{\pi}{16} \frac{1}{F} I_d^2 \tag{11}.$$

The correction factor F was determined for every sample film.

A comment upon the calculation of the correction term in Eq. (4) is made here. In Fig. 4 values of M_{ex}/M_∞ at 0.5, 1, 2, 4, and 9 minutes, for the system of xenon and L-1 calculated by using Eqs. (8) and (11) are plotted against $t^{1/2}$. It is seen that the plots for short times, as indicated by the filled circles, are well approximated by a straight line which passes the origin. This suggests that the short-time exhaust process, two-minutes exhaust for the example given in the figure, is controlled dominantly by the diffusion mechanism and that the correction factor in Eq. (4) may be satisfactorily evaluated by using the relations for diffusion described in the foregoing lines.
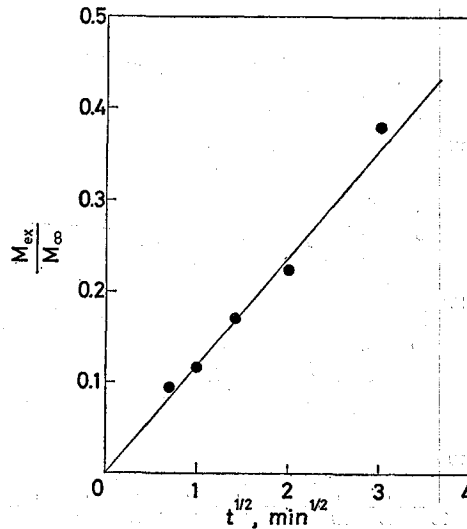

Fig. 4. Variation of M_{ex}/M_∞ with exhaust time. Desorption of xenon from L-1 at 25°C.

RESULTS

Solubilities $S(p_0) \cdot p_0$ of argon in the samples R-1 and L-1 at 25°C are plotted against pressure p_0 in Fig. 5. The plots for both block copolymer samples can be represented by a single straight line which passes the origin. This shows that the
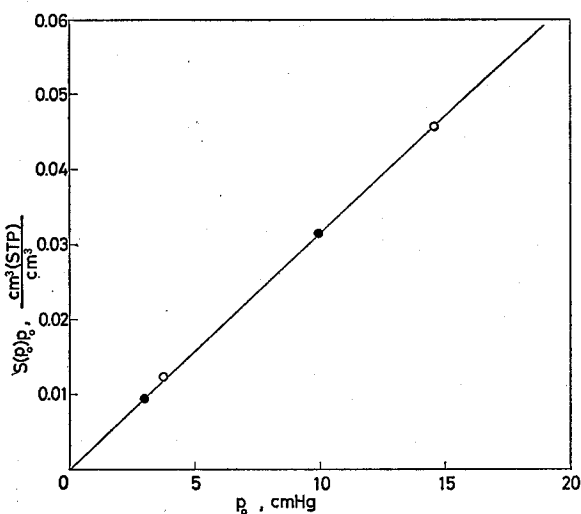
Fig. 5. Solubility of argon at 25°C as a function of pressure of the gas. SBS block copolymers: ●, R–1; ○, L–1.
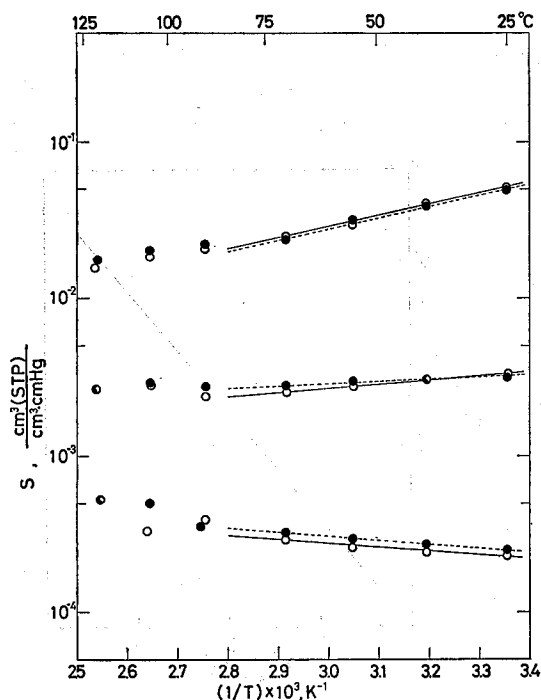

Fig. 6. Temperature dependence of equilibrium solubility coefficient S. SBS block copolymers: ●, R–1; ○, L–1. Gases: upper, Xenon; middle, Argon; lower, Helium.

Henry's law is obeyed by the systems and hence the solubility coefficient is independent of the penetrant pressure in the region of pressure studied. Quite the same behavior was observed for the solution of helium and xenon in the block copolymer samples. Accordingly, a symbol S replaces $S(p_0)$ hereafter to express the pressure-independent solubility coefficient. The time-lag solubility coefficient S_θ was found also to be

independent of pressure for all systems studied.

Figure 6 shows the temperature dependence of the equilibrium solubility coefficient. The precision of the solubility coefficient was $\pm 3\%$ at the 95% confidence level. As has been observed for the temperature dependence of the permeability and the (time-lag) diffusion coefficients reported in Part I, the temperature dependence of S in the temperature region lower than about 85°C is expressed by the Arrhenius-type equation

$$S = S_0 \exp\left(-\Delta H_s / RT\right) \tag{12}.$$

Here ΔH_s is the apparent heat of solution. The values of ΔH_s determined are given in Table I. The uncertainty in ΔH_s is estimated to be ± 0.6 kJ. No substantial difference is observed in ΔH_s for the solution of gases in the two block copolymer samples having different types of domain structure.

Figures 7 (a) and (b) show the temperature dependence of the time-lag solubility coefficient for the solution of argon and xenon in the copolymer samples, respectively. In the figures the data of S are plotted for the sake of comparison. The precision of solubility coefficients determined by the time-lag method was worse than that of S, and was $\pm 10\%$ at the 95% confidence level. Furthermore, fairly large scatterings (indicated by vertical bars) were sometimes observed if measurements were made with different sample films. Solubility coefficients, S and S_θ, at 25°C are compared

Table I. Apparent Heats of Solution. ΔH_s in kJ/mol

Gas	ΔH_s	
	R–1	L–1
He	5.0	4.6
Ar	−2.1	−5.0
Xe	−14.2	−14.2
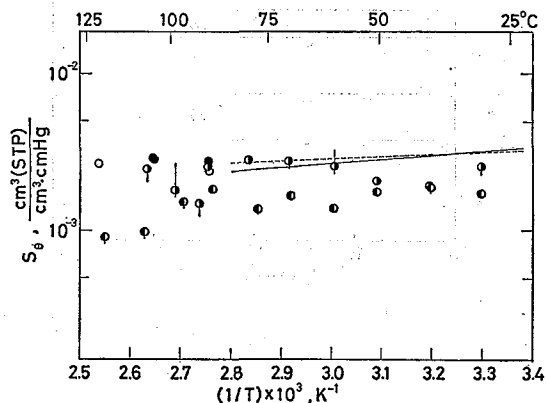
Fig. 7 (a). Temperature dependence of time-lag solubility coefficient S_θ.

SBS block copolymers	R–1	L–1
S_θ	◖	◑
S	----●----	──○──

Gas: Argon.
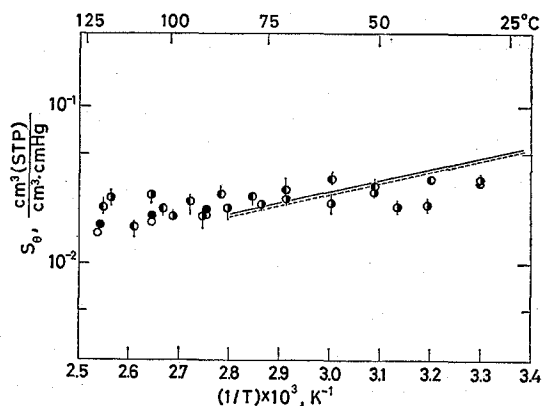
Fig. 7 (b).   Xenon.

Table II.   Solubility Coefficients at 25°C. S, S_θ, and $v_B S_B$ in $cm^3(STP)/(cm^3 \cdot cm\ Hg)$

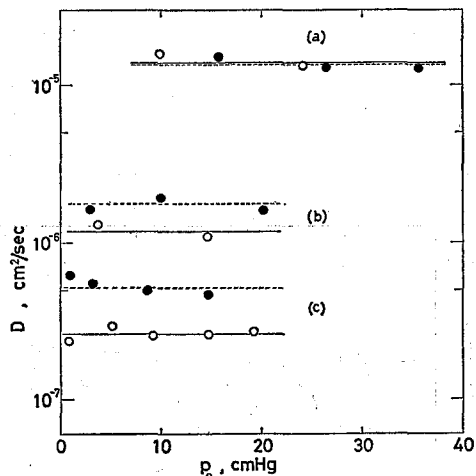| Gas	S		S_θ		$v_B S_B$	
	R-1	L-1	R-1	L-1	R-1	L-1
He	$2.5_4 \times 10^{-4}$	$2.3_1 \times 10^{-4}$	—	—	—	—
Ar	$3.1_6 \times 10^{-3}$	$3.2_9 \times 10^{-3}$	2.2×10^{-3}	1.9×10^{-3}	2.5×10^{-3}	2.1×10^{-3}
Xe	$4.9_4 \times 10^{-2}$	$5.1_0 \times 10^{-2}$	3.5×10^{-2}	3.6×10^{-2}	3.6×10^{-2}	3.0×10^{-3}

Fig. 8.   Diffusion coefficient at 25°C as a function of pressure of gas.   SBS block
copolymers: ●, R-1; ○, L-1.   Gases: (a) Helium; (b) Argon; (c) Xenon.

with each other in Table II.   The equilibrium values are always greater than the cor-
responding time-lag values.

The dependence of D on p_0 is shown in Fig. 8.   It is seen that D is independent
of pressure within the region studied.   The similar behavior was observed at any
other temperature studied.   Since the Henry's law is obeyed by all the systems studied
as described above, it follows that D does not depend on penetrant concentration.

The result shown in Fig. 8 assures, therefore, that the mutual diffusion coefficients of the systems concerned have been determined by the procedure described in the preceding section. It was observed that the time-lag diffusion coefficient was also independent of p_0, and hence of penetrant concentration, in the region studied.

Table III gives data of the diffusion coefficients at 25°C. The precision of diffusion coefficients determined by the desorption and time-lag methods were respectively $\pm 5\%$ and $\pm 8\%$ at the 95% confidence level. Diffusion coefficients for the sample L–1 are less than those for R–1, and the differences between values of the two sets of diffusion coefficient are not so great as those of the solubility coefficients. The temperature dependence of the diffusion coefficient determined by the desorption method was well expressed by the Arrhenius-type equation with constant E_D as in the case of the time-lag diffusion coefficient,[1] where E_D is the apparent activation energy for diffusion. Again, linear Arrhenius plot was limited to in the temperature region lower than about 85°C. Table IV gives the apparent activation energies for diffusion evaluated from the desorption experiments.

Table III. Diffusion Coefficients at 25°C. D and D_θ in cm²/sec

Gas	D		D_θ	
	R–1	L–1	R–1	L–1
He	1.53×10^{-5}	1.31×10^{-5}	—	—
Ar	1.94×10^{-6}	1.30×10^{-6}	1.75×10^{-6}	1.14×10^{-6}
Xe	5.5×10^{-7}	2.6×10^{-7}	5.6×10^{-7}	2.8×10^{-7}

Table IV. Apparent Activation Energies for Diffusion. E_D in kJ/mol

Gas	E_D	
	R–1	L–1
He	17.6	16.3
Ar	23.0	24.7
Xe	28.6	35.1

DISCUSSION

Solubility Coefficients.

From Fig. 7 and Table II it is seen that, for argon and xenon at lower temperatures, the equilibrium solubility coefficients are greater than the time-lag solubility coefficients. The equilibrium solubility coefficients of inert gases in polybutadiene (of high cis-isomer content) are not different much from those in polystyrene.[8] On the other hand, the diffusion coefficients of inert gases in glassy polystyrene are much smaller than those in rubbery polybutadiene. Accordingly, the difference between two solubility coefficients suggests that the time-lag method counts only the mobile gas molecules in the polybutadiene matrix, while the desorption method counts less diffusive species in the glassy polystyrene domains as well. The difference between S and S_θ becomes less apparent with increasing the temperature of experiments.

(419)

In the temperature region above about 85°C, which is close to the glass transition temperatures of polystyrene blocks in the copolymer samples R–1 and L–1,[1] both plots seem to merge in a single curve though the results, especially those of S_θ for argon, scatter markedly in the temperature region.

If the time-lag solubility gives only the concentration of gas molecules in the polybutadiene matrix as suggested in the preceding paragraph, the values of S_θ should be well compared with those of a product $v_B S_B$, where v_B is the volume fraction of butadiene component of the block copolymer sample and S_B the solubility coefficient of the gas in polybutadiene. For the solution of argon and xenon, values of the product $v_B S_B$ were calculated using the observed values of S_B, which was measured with polybutadiene of nearly the same isomer content as polybutadiene blocks of the samples R–1 and L–1. The results are given in the fifth and sixth columns of Table II. The calculated values of the product $v_B S_B$ are in good agreement with observed values of S_θ. This may be considered to confirm the view mentioned above.

Michaels and Bixler have demonstrated that the logarithm of the solubility coefficient of inert gases in polyethylene is linearly correlated with the Lennard-Jones force constant of the gases.[9] Similar results have been obtained for the solution of inert gases in poly(ethylene terephthalate),[10] copolymer of hexafluoropropylene and tetrafluoroethylene,[11] and poly(methyl methacrylate).[12] Also, a theoretical basis of the linear relationship has been given by them through a thermodynamic analysis.[9] In Fig. 9 are plotted similogarithmically the equilibrium solubility coefficient at 25°C, S_{25}, against the Lennard-Jones force constant, ε/k. The data for nitrogen solubility, which will be reported in detail in a forthcoming article, are also included in the figure. The fit to a straight line is good, and the straight line is expressed by the equation

$$ln \; S_{25} = 0.025 \, \varepsilon/k - 3.66 \qquad\qquad (13).$$

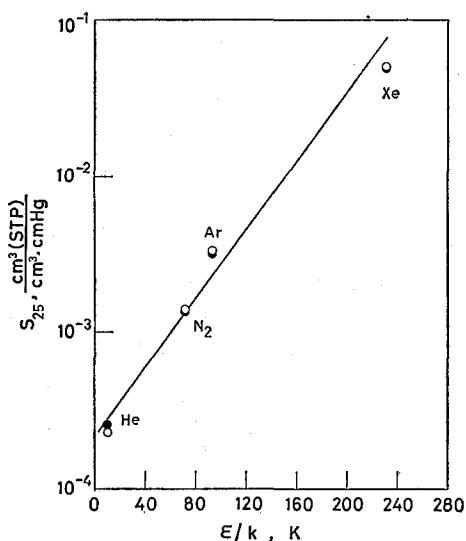Fig. 9. Logarithm of equilibrium solubility coefficient at 25°C, S_{25}, of four gases as a function of the Lennard-Jones force constant, ε/k. SBS block copolymers: ●, R–1; ○, L–1.

The slope of the line is in excellent agreement with that, 0.026, predicted by Michaels and Bixler through the thermodynamic treatment, and also is well compared with that, 0.022, for the system of polyethylene and inert gases.[9]

The solution process of a gas in the polymer may be considered to occur in two successive steps; the first is the condensation of the gas and the second is the mixing of the condensed gas with the polymer. Accordingly, the apparent heat of solution may be written as

$$\Delta H_s = \Delta H_c + \Delta H_m \tag{14},$$

where ΔH_c is the heat of condensation and ΔH_m the heat of mixing. For gases above their critical points ΔH_c is negligible and

$$\Delta H_s \cong \Delta H_m \tag{15}.$$

For helium the apparent heat of solution is therefore small and positive. With increasing the size of the penetrant molecule, greater energy is needed to form the hole, in which the penetrant molecule is accomodated, in the polymer matrix and ΔH_s becomes negative. The data given in Table I harmonize well with this view. Also, the data indicate that ΔH_s, and hence ΔH_m, is not influenced much by the variation in the domain structure of the block copolymer sample.

Using the same thermodynamic model as used in the derivation of the relationship between the solubility coefficient and the Lennard-Jones force constant, Michaels and Bixler[9] found that the heat of solution should be given by

$$\Delta H_s = \chi RT - 0.0653 \varepsilon/k \tag{16},$$

where χ is the mixing parameter. Figure 10 shows the plot of ΔH_s, which is determined at lower temperatures, versus ε/k. Again, it can be seen that the plot is well represented by a straight line having the slope of 0.087, which is close to the predicted value 0.0653. Thus, the solution behavior of inert gases in the SBS block copolymer seems to be explained satisfactorily by the thermodynamic treatment developed by Michaels and Bixler.
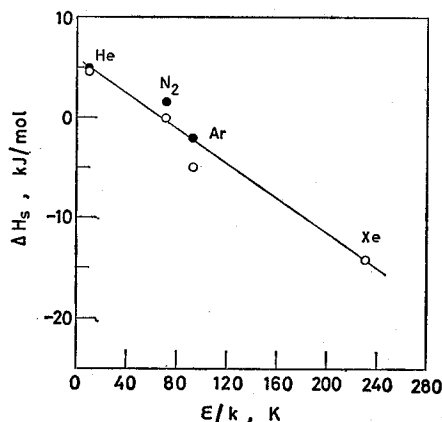

Fig. 10. Apparent heat of solution, ΔH_s, of four gases as a function of the Lennard-Jones force constant, ε/k. SBS block copolymers: ●, R–1; ○, L–1.

Diffusion Coefficients.

As shown in Table III the observed values of the two sets of diffusion coefficient are practically the same. Therefore, it may be concluded that the polybutadiene phase in the block copolymer, which governs mostly the permeation behavior in the transient state, is also responsible for the desorption process of the inert gas from the SBS block copolymer solid.

In Part I, two impedance factors τ and β were introduced in order to explain the observed selectivity for permeation to gases, having different molecular size, through the block copolymer. Here, τ and β are the tortuosity factor and the chain im-mobilization factor, respectively. The product $\tau\beta$ was estimated from the observed permeability, and it was found that the values of $\tau\beta$ for the sample R–1 was close to unity, while those for the sample L–1 was greater than unity and increased with increasing the molecular size of the gas.

The product $\tau\beta$ can be evaluated alternatively from the diffusion coefficient. If D_B denotes the diffusion coefficient for homopolybutadiene, it follows from the defini-tion of the factors τ and β that

$$D = \frac{D_B}{\tau\beta} \tag{17},$$

or

$$D_\theta = \frac{D_B}{\tau\beta} \tag{18}.$$

The product $\tau\beta$ may also be estimated from the observed values of P and S_B, where P is the permeability coefficient of the gas in the block copolymer. As described in Part I, if the molecular size of an inert gas is not so small as that of helium, P can be ex-pressed as

$$P = v_B P_B \tag{19},$$

since the diffusion coefficient for polybutadiene is fairly greater than that for polystyrene, where P_B is the permeability coefficient of polybutadiene. By dividing by $v_B S_B$, the diffusion coefficient for the polybutadiene phase in the SBS block copolymer, D_B^*, is given by

$$D_B^* = \frac{P}{v_B S_B} \tag{20}.$$

The correlation between D_B^* and D_B is then given by

$$D_B^* = \frac{D_B}{\tau\beta} \tag{21}.$$

Table V. Estimated Products of the Tortuosity Factor, τ, and the Chain-immobiliza-tion Factor, β, at 25°C

			$\tau\beta$			
	From D_B/D		From D_B/D_θ		From D_B/D_B^*	
Gas	R–1	L–1	R–1	L–1	R–1	L–1
He	1.0[a]	1.2[a]	—	—	—	—
Ar	1.1	1.7	1.3	2.0	1.4	2.1
Xe	1.4	3.1	1.4	2.8	1.4	2.4

[a] D_B from data of Bixler and Sweeting.[13]

The estimated products of $\tau\beta$, for which the data obtained at 25°C was used, are shown in Table V. Though the values of $\tau\beta$ thus estimated are somewhat larger than those from the permeability data,[1] it is apparent without any doubt that the product increases with increasing the molecular size of the gas and that the products for L–1 are greater than those for R–1 for all gases studied. Thus, the result given in the table seems to suggest again that the chain immobilization factor β for the sample L–1 increases with increasing the size of penetrant molecule.

REFERENCES

(1) H. Odani, K. Taira, N. Nemoto, and M. Kurata, *This Bulletin*, **53**, 216 (1975).

(2) P. Meares, *Trans. Faraday Soc.*, **54**, 40 (1958).

(3) A. S. Michaels and R. B. Parker, Jr., *J. Phys. Chem.*, **62**, 1604 (1958).

(4) J. Crank, "Mathematics of Diffusion", Oxford Univ. Press, London, 1956, Chap. 4.

(5) Ref. (4), Chap. 11.

(6) (a) Ref. (4), Section 2.5; (b) H. S. Carslaw and J. C. Jaeger, "Conduction of Heat in Solids", 2nd Ed., Oxford Univ. Press, London, 1959, Chap. 4.

(7) A. S. Carpenter and D. F. Twiss, *Ind. Eng. Chem., Anal. Ed.*, **12**, 99 (1940).

(8) Unpublished results in our laboratory.

(9) A. S. Michaels and H. J. Bixler, *J. Polym. Sci.*, **50**, 393 (1961).

(10) A. S. Michaels, W. R. Vieth, and J. A. Barrie, *J. Appl. Phys.*, **34**, 1 (1963).

(11) R. A. Pasternak, G. L. Burns, and J. Heller, *Macromolecules*, **4**, 470 (1971).

(12) V. M. Patel, C. K. Patel, K. C. Patel, and R. D. Patel, *Makromol. Chem.*, **158**, 65 (1972).

(13) H. J. Bixler and O. J. Sweeting in "The Science and Technology of Polymer Films", vol. 2, O. J. Sweeting Ed., Wiley-Interscience, Inc., New York, 1971, Chap. 1, Appendix Table 1.